New attenuation correction for the HRRT using transmission scatter correction and total variation regularization

Merence Sibomana, Sune Høgild Keller, Claus Svarer, Oline Vinter Olesen, Flemming Andersen, Søren Holm and Liselotte Højgaard

I. Introduction

In the standard software for the Siemens HRRT PET scanner the most commonly used segmentation in the μ-map reconstruction for human brain scans is MAP-TR. Problems with bias in the lower cerebellum and pons in HRRT brain images have been reported. The main source of the problem is poor bone / soft tissue segmentation in these regions and the lack of scatter correction in the μ-map reconstruction. In this paper we describe and validate the new TXTV segmentation method (included in the HRRT_U 1.0 and 1.1 user software) aimed at solving the bias problem.

Its improvements fall in two parts: Firstly, it introduces the use of scatter correction, and secondly, it uses a simple threshold in combination with nonlinear total variation μ-map filtering.

To validate the new transmission μ-map reconstruction with scatter correction and TXTV segmentation, we compared the average activity in 50 RoIs average on emission images reconstructed with the new TXTV and old MAP-TR μ-maps to images reconstructed with co-registered CT-based μ-maps on four 18F FDG scans. The CT μ-maps is considered a gold standard. The comparison show a significant decrease in the bias in cerebellum and pons, and a better agreement between images reconstructed with the new method and CT-based μ-maps.

II. Methods

The HRRT transmission scan uses a ^{137}Cs source at 662KeV.

A. Old Method:MAP-TR

The current method [1] histograms the reconstructed μ-map to find peaks (assuming that most pixels are water) and applies a global scaling factor to all pixels to get the peak pixel values to fit the water mu-value at 511KeV (0.096 cm^{-1}). The scaling is used to correct for both energy difference and scatter.

B. New Method: TXTV

1) Scatter Correction

We have implemented the scatter correction developed for the ECAT ART [2]. The old equation to find the attenuation correction factor (ACF) in the iterative reconstruction of the μ-map is $ln(ACF) = ln(bl/tx)$ where tx is the transmission scan and bl is a blank scan. The new equation used is

$$\ln(ACF) = a + b * \ln\left(\frac{bl}{tx}\right)$$

where values of the constants a and b were adjusted using three high statistics transmission scans (25min. each) of cylinder phantoms of different diameters (2, 10 and 20cm) filled with water to obtain the expected mu value of 0.086 cm^{-1} at 662KeV. The absolute scaling factor **1.116** (0.096/0.086) was applied to get the μ-value at 511KeV.

2) Segmentation

The replacement for MAP-TR, named TXTV(3Dreg) is not a traditional complete segmentation, it is a combined partial thresholding and nonlinear regularization (smoothing). The unsegmented HRRT μ-maps (size: 128×128×207) are noisy and contain underestimated pixels in the center of the brain tissue due to residual scatter although the new scatter correction reduces this effect. The initial threshold process raises underestimated tissue pixels in the range [0.07, 0.099] to the tissue mu-map value of 0.099. The images are still noisy and needs filtering.

3) Nonlinear Filtering

The classic choice would be to use Gaussian smoothing, but to preserve the bone segmentations below the brain and general sharp edges, we chose to use the nonlinear total variation (TV) regularization. Nonlinear filtering is normally considered slow, but sufficiently smoothed μ-maps were produced in less than five seconds on a standard laptop.

Total variation preserves structures and edges/boundaries in images while still removing noise, and the filtering is done using an iterative solver. Iterating TV regularization too far starting from a noise-free (photographic) image will often result in a cartoon-like image with flat plateaus separated by sharp edges, which is also the desired look of a well-segmented μ-map. Modeling the regularization as an energy minimization problem, TV can be formulated as

$$E(u) = \int_\Omega (u - u_0)^2 dx + \lambda \int_\Omega \psi(|\nabla_3 u|) dx$$

where u_0 is the input image and u the regularized output. Ω is the domain of our TX image, x denotes the position in the image, λ is the weight controlling the degree of smoothing and ∇_3 is the 3D local spatial gradient operator. Since the function $|\cdot|$ is not differentiable at the origin, we replace it by the approximation $\psi(x) = \sqrt{x^2 + \varepsilon^2}$, with ε = 0.01. The second term of the energy is the TV smoothing term (model term), which would become Gaussian if the gradient was squared. The first term is a reaction term (data term), which controls the degree of smoothing relative to the input image (through the size of λ). By using calculus of variation we obtain the Euler-Lagrange equation

$$\frac{\partial E(u)}{\partial u} = (u - u_0) - \lambda \mathrm{div}_3\left(\frac{\nabla_3 u}{\psi(|\nabla_3 u|^2)}\right) = 0$$

where div_3 is the 3D divergence operator. This nonlinear equation is solved using a fixed point scheme: The nonlinear

parts are updated a number of times (outer iterations). After each update they are fixed while a linear Gauss-Seidel solver is used on the now linear system. The new value of each pixel is found from (1) with the A's being the nonlinear parts that are kept constant during the inner iterations. The indexes in (1) denotes the compass directions **w**est, **e**ast, **n**orth and **s**outh, and **b**efore and **a**fter. The nonlinear parts (the A's) only updated only in the outer iterations are directional symmetric, and from the example of A-west given in (2) the remaining are easily found. For details on implementation and in-depth theory we refer to [3] and [4].

C. Validation

Standard statistics transmission scans (6 min.) and 40 min. ^{18}F FDG emission scans of four volunteers were acquired on the HRRT and CT images of the same subjects were also acquired. CT-derived μ-maps were calculated and registered to the HRRT μ-maps using Vinci 2.50 [6]. Four each subject three emission images where reconstructed using a) the "gold standard" CT-based μ-map, b) the TXTV μ-map and c) the MAP-TR μ-map. A probability based automatic delineation of volumes of interest [5] was used to delineate 50 RoIs on MR images of each subject, which were registered to the HRRT emission images. The activity mean in each of the RoIs in the EM reconstructions (10 iterations OP-OSEM3D with PSF resolution modeling [7]) where then compared: CT μ-map vs. MAP-TR μ-map and CT vs. TXTV μ-map.

III. Results

A. Scatter Correction Parameters from Phantom Scans

The new HRRT μ-map reconstruction was used on two high statistics transmission scans (speed=10, step=2, 25min) of a 20cm cylinder phantom filled with water and the HRRT QC phantom; a 20cm cylinder phantom filled with ^{68}Ge epoxy. The μ-maps were uniform and the average value with absolute scaling was respectively 0.096 and 0.103 as expected at 511KeV. Two smaller water phantoms (D = 10cm and D = 2cm) were also scanned with the same settings and used to adjust the scatter correction parameters by computing the ratio between a central RoI (D = 8cm) and an annulus (inner D = 16cm, outer D = 18 cm) on the 20cm phantoms. The parameter a was used to adjust the shape of the radial profile, whereas b was used to adjust the RoI average to the expected value and finally set to b = 1.18. Setting a = -0.14 gave an excellent ratio (1.0 for the 20cm water phantom and 0.99 for the germanium phantom). However, a = -0.1 gave a better agreement between the three water phantoms for their profiles, and the ratios were 0.977 for the 20cm water phantom and 0.973 for the germanium phantom.

B. Human Brain Scans

Fig. 1 shows μ-maps for one of the four subjects scanned in this study. The CT-based μ-map (top right) is used as a gold standard. Running TXTV on the scatter corrected μ-map (top left) result in a μ-map (bottom left) which is close to the "gold standard" CT μ-map, and in comparison to standard HRRT MAP_TR μ-maps (not shown), more bone is visible below the brain. The profiles (bottom right) shows that TXTV still has slightly varying brain tissue values as compared to the CT μ-map (and MAP-TR μ-map).

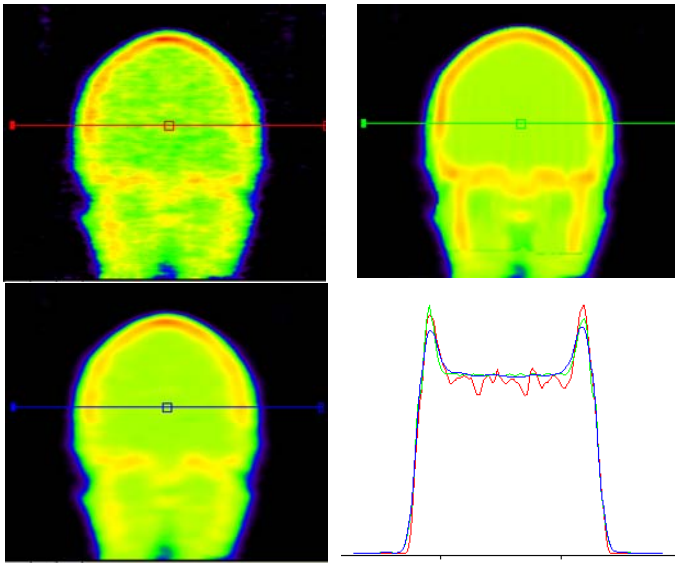

Fig. 1. Top: Unsegmented, scatter corrected HRRT μ-map left and CT-based μ-map right. Bottom: TXTV μ-map and horizontal profiles for the μ-maps.

C. Validation Against "Gold Standard" CT μ-maps on Emission Images

To evaluate the bias in using the old (MAP-TR) and new (TXTV) μ-maps we compared the mean activities in the 50 RoIs in each of the four subject emission reconstructions. In all four subjects the ratio of EM means with HRRT μ-map over EM means with CT μ-map is significantly larger with the old MAP-TR HRRT μ-map than with the new TXTV HRRT μ-map. Fig. 2 shows the ratios of 1 – (EM mean HRRT / EM mean CT) for all 50 RoIs in the four subjects. It is clear to see that using the new TXTV μ-map (right) significantly lowers the bias compared to using the old MAP-TR μ-map.

$$u_c = \frac{\lambda(A_w \cdot u_w + A_e \cdot u_e + A_n \cdot u_n + A_s \cdot u_s + A_a \cdot u_a + A_b \cdot u_b) + u_{0,c}}{\lambda(A_e + A_w + A_n + A_s + A_a + A_b) + 1} \tag{1}$$

$$A_w \approx \frac{1}{\sqrt{(u_w - u_c)^2 + \frac{1}{16}(u_n - u_s + u_{nw} - u_{sw})^2 + \frac{1}{16}(u_a - u_b + u_{aw} - u_{bw})^2 + \varepsilon^2}} \tag{2}$$

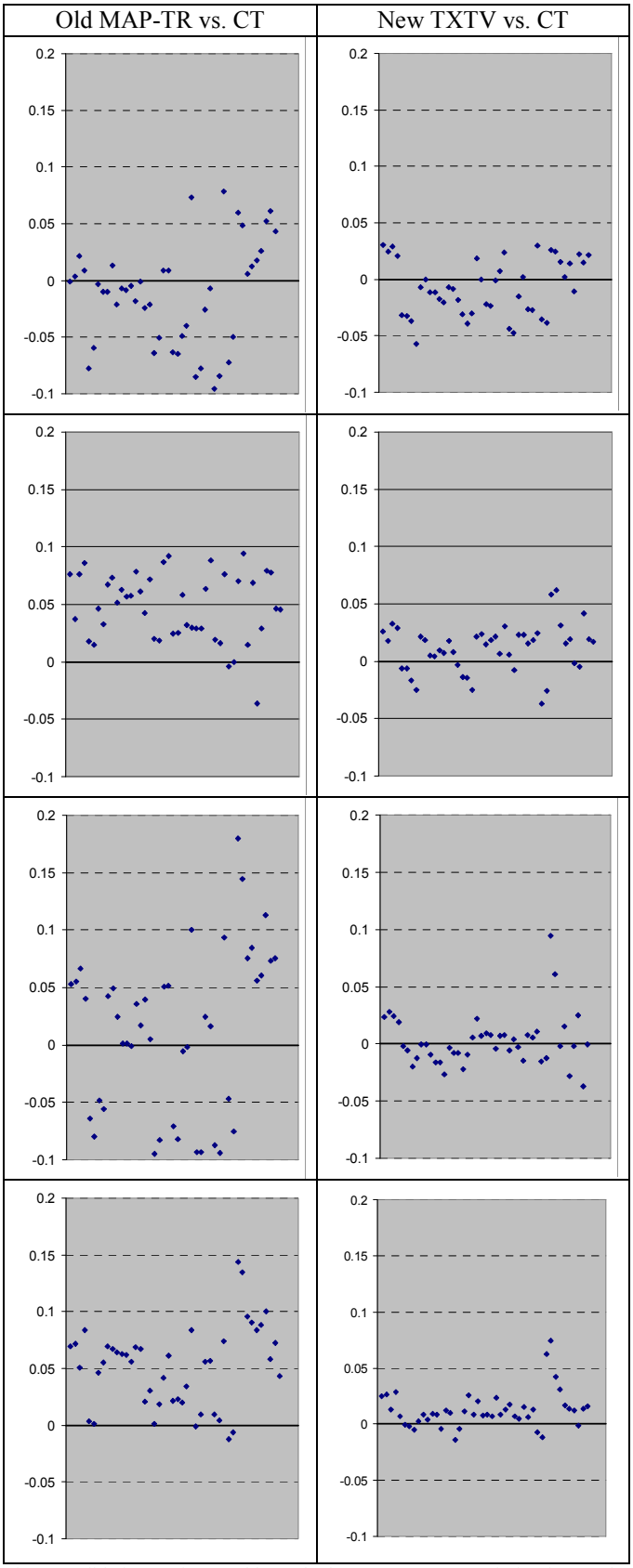

Fig. 2. Validation against "gold standard" CT μ-maps on emission images by mean values in the 50 RoIs. Left column: Old MAP-TR vs. CT. Right column: New TXTV vs. CT. Each row represents a subject. It is clear that the TXTV values in the in the right column are closer to the CT values than the MAP-TR values in the left column

IV. Discussion

In order to lower the bias even more, we tried to extend the threshold process to the range between brain tissue and bone and do additional morphological opening before the TV regularization, but all attempts resulted in the loss of the bone below the brain and gave higher bias (in the range of the MAP-TR bias).

Thus it seems we need to add additional information to further improve the HRRT μ-maps. One option is to use brain atlas modeling, another is MR based μ-maps, which we will investigate in the future. Many subjects already get an MR scan used for segmentation, and the bone/air segmentation problem often encountered in PET-MR μ-map reconstruction could be (at least partially) avoided by using the HRRT TX scan data.

TVTX has also been validated on an ^{18}F-Altanserin study [8]: The four subjects in that study were scanned both on the HRRT and on a GE Advance PET scanner showing comparable results between the two scanners when using TXTV (this was not the case when using MAP-TR).

References

[1] M. Sibomana *et al.*, Simultaneous measurement of transmission and emission contamination using a collimated 137Cs point source for the HRRT, IEEE MIC Record, Roma, 2004.

[2] C. Watson *et al.*, Design and performance of a single photon transmission measurement for the ECAT ART, IEEE NSS Record, Albuquerque, 1997.

[3] L. Rudin, S. Osher, and E. Fatemi, Nonlinear total variation based noise removal algorithms, *Physica D*, vol. 60, pp. 259–268, 1992.

[4] S. H. Keller Video Upscaling Using Variational Methods, Ph.D. dissertation, Faculty of Science, University of Copenhagen, 2007. [Online]. Available: http://image.diku.dk/sunebio/Afh/SuneKeller.pdf

[5] C. Svarer, K. Madsen, S. G. Hasselbalch, L. H. Pinborg, S. Haugbol, V. G. Frokjaer, S. Holm, O. B. Paulson, and G. M. Knudsen. MR-based automatic delineation of volumes of interest in human brain PET images using probability maps. Neuroimage 24 (4):969-79, 2005.

[6] Vinci, Volume Imaging in Neurological Research, Co-Registration and ROIs Included, http://www.nf.mpg.de/vinci/index2.html

[7] C. Comtat *et al.*, Image based resolution modeling for the HRRT OSEM reconstruction software, IEEE MIC Record, Dresden, 2008.

[8] C. Svarer *et al.*, HRRT and Advance scanner comparison using a steady-state scan approach, SNM, Toronto, 2009.